Colloids and Surfaces B: Biointerfaces 241 (2024) 114063

Contents lists available at ScienceDirect

Colloids and Surfaces B: Biointerfaces

journal homepage: www.elsevier.com/locate/colsurfb

From adsorption to crystallization of proteins: Evidence for interface-assisted nucleation

Hadra Banks [a,*], Furio Surfaro [a], Kai-Florian Pastryk [a], Cara Buchholz [a], Ivan A. Zaluzhnyy [a], Alexander Gerlach [a], Frank Schreiber [a,b]

[a] Institut für Angewandte Physik, Universität Tübingen, Auf der Morgenstelle 10, Tübingen 72076, Germany
[b] Center for Light-Matter Interaction, Sensors & Analytics LISA+, Auf der Morgenstelle 15, Tübingen 72076, Germany

ARTICLE INFO

Keywords:
Protein crystallization
Heterogeneous nucleation
Human serum albumin
Protein adsorption
QCM-D

ABSTRACT

Protein crystallization is among the key processes in biomolecular research, but the underlying mechanisms are still elusive. Here, we address the role of inevitable interfaces for the nucleation process. Quartz crystal microbalance with dissipation monitoring (QCM-D) with simultaneously optical microscopy, confocal microscopy, and grazing-incidence small angle X-rays scattering (GISAXS) were employed to investigate the temporal behavior from the initial stage of protein adsorption to crystallization. Here we studied the crystallization of the Human Serum Albumin (HSA), the most abundant blood protein, in the presence of a charged surface and a trivalent salt. We found evidence for interface-assisted nucleation of crystals. The kinetic stages involved are initial adsorption followed by enhanced adsorption after longer times, subsequent nucleation, and finally crystal growth. The results highlight the importance of interfaces for protein phase behavior and in particular for nucleation.

1. Introduction

Understanding protein phase behavior is fundamental to many fields of science such as tissue engineering, drug delivery, medicine, structural biology, food processing and protein-related diseases [1–3]. The knowledge of protein structure is essential to understand their functions and behavior [4]. Obtaining protein crystals is crucial as crystallography is extensively used to resolve protein structures [5]. However, many proteins are not yet crystallized, and the strategy employed is often through trial and error which is rather inefficient [6]. Therefore, it is essential to understand the mechanisms behind protein crystallization. Several theories have been put forward on protein crystallization [7–10, 11,12] and it emerged that the situation is frequently more complex than the simple classical nucleation theory (CNT) [8,13–15].

A point which is usually not being considered is the presence of interfaces in any real experiment. Here, we address two main questions regarding protein crystallization and protein-surface interaction: where is the site of nucleation and what mechanisms are behind such phenomena. Human serum albumin (HSA), the most abundant blood protein [16,17], was used as a model system to investigate protein crystallization at a negatively charged surface (glass or SiO_2). Surface-sensitive techniques such as quartz crystal microbalance with dissipation monitoring (QCM-D) with simultaneous optical microscopy and grazing-incidence small angle X-rays scattering (GISAXS) were employed to follow the process of adsorption, enhanced adsorption and crystallization.

2. Results

2.1. Protein-protein interactions

HSA is net negatively charged at neutral pH [17–20]. Thus, without addition of salt or at low salt concentration (c_s), the proteins repel each other. In the phase diagram this is called regime I. Upon further increase of the trivalent salt c_s, a pseudo phase boundary is reached (c^*) where attractive interactions are dominant in what is called regime II [21]. This value (c^*) is the concentration of salt, at a given protein concentration (c_p), where the solution becomes turbid. For HSA with $LaCl_3$, the value of c^* at $c_p = 60$ mg/ml is 4.42 mM. At higher c_s, a second pseudo phase boundary is crossed (c^{**}), where a charge inversion at the surface of proteins occurs as a result of screening cations; hence, repulsive forces are dominant again in regime III. This phenomenon is called re-entrant

* Corresponding author.
E-mail address: hadra-sioux.banks-machado@uni-tuebingen.de (H. Banks).

https://doi.org/10.1016/j.colsurfb.2024.114063
Received 5 March 2024; Received in revised form 26 April 2024; Accepted 25 June 2024
Available online 28 June 2024

condensation [21,22]. The complete phase diagram is shown in Fig. S1. The protein behavior can be modeled by an ion-activated mechanism for patchy interaction where specific binding and bridging takes place between La^{3+} and protein molecules [23]. For a more detailed account of multivalent ions and biomolecules we refer to Ref. [24].

To characterize protein-protein interactions and predict good conditions for crystallization [25,26], the second virial coefficient (B_2) was determined [27]. This value is related to the pair interaction potential between particles and is negative if the dominating interaction is attractive and positive if repulsive [28]. HSA shows a negative value of $B_2/B_2^{HS} = -1.97$ (normalized to the B_2 of hard spheres) measured at c^*, indicating that this region is dominated by attractive interactions. Additionally, the value is inside the crystallization slot, predicting ideal conditions for crystal growth [29,30].

2.2. From adsorption to crystallization

In order to elucidate the role of the interface for crystallization, we investigate protein adsorption during time under crystallization conditions. Figure 1 a) shows changes of frequency ($\Delta f3$), b) dissipation ($\Delta D3$) measured with QCM-D and the c) respective simultaneously acquired microscopy images from the quartz sensor surface, as in this experimental setup we are able to have optical access to the sensor surface trough a sapphire window. The negative frequency shift does not saturate within the first hour as expected for normal protein adsorption, but rather sharply decreases within the first minutes due to the contact of the protein solution with the surface, and continuously decreases over time, indicating that proteins are still adsorbing after the first hour. This is called enhanced adsorption, where a multilayer of proteins is forming at the surface [31]. The dissipation also continuously increases, showing that the adsorbed layer is also becoming softer [32]. Furthermore, an interesting frequency shift was observed. The frequency change (Fig. 1a) highlighted in the inset) shows an 'anti-Sauerbrey' behavior, where

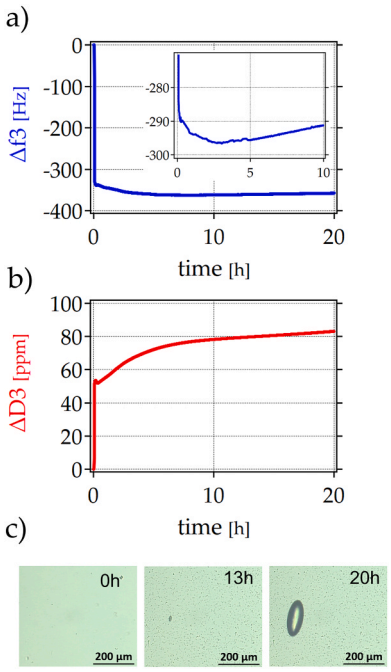

Fig. 1. QCM-D a) frequency and b) dissipation curves and the respective c) microscope images showing HSA adsorption, nucleation and crystal growth for $c_p = 80$ mg/ml; $c_s = 6.1$ mM. An anti-Sauerbrey frequency shift and increase in dissipation is observed after enhanced adsorption and before crystallization, suggesting that nucleation is taking place within the multilayer, as a transformation of the layer is present before crystals are visible. For a video showing QCM-D and microscopy data, see supplementary material.

despite the positive frequency shift there was no change in the total mass inside the QCM-D chamber (i.e washing or adding solution). An anti-Sauerbrey behavior was previously observed for other systems [33–36,37]. Additionally, we observed the same characteristic dependency of frequency and dissipation over time in another protein-salt system during crystallization, i.e. β-lactoglobulin (BLG) with $LaCl_3$ (Fig. S2). The primary causes of such a behavior are related to transformations within the multilayer such as changes in the viscoelastic properties during the measurement and the increase of the layer thickness over time [33,37]. The turning point of the frequency shifts corresponding to an anti-Sauerbrey behavior is around three hours and thirty minutes. After this point the frequency continues to increase, in contrast to only enhanced adsorption without crystal nucleation, where the frequency continuously decreases.

Protein-surface interaction leads to a sharp decrease of the frequency over time, then enhanced adsorption continuous for around 3 h during which a multilayer was formed. Before crystals are visible under the microscope, the adsorbed layer becomes softer and the frequency shifts towards positive values, indicating a transformation within the adsorbed layer. Around 7 h later crystals are visible under the microscope. The layer transformation observed by QCM-D before crystals are visible, suggesting that nucleation is happening within the adsorbed multilayer.

As protein adsorption seems to be connected to protein crystallization, we investigate the correlation between protein adsorption and crystal density. The conditions are chosen such that the strength of interaction is constant, using constant c_s/c_p. The adsorbed layer thickness of HSA with $LaCl_3$ on the surface is shown in Fig. 2a). After two hours of adsorption a multilayer (enhanced adsorption) is formed for all protein concentrations tested. The multilayer thickness increases with increasing protein concentration, similar to Ref. [31]. Additionally, we found that with increasing protein concentration, the softness of the layer increases. A higher dissipation (Fig. 2b)) is associated with softer layers.

In order to investigate the properties of the multilayer, after two hours of adsorption the surface was rinsed with the solvent for 10 min, so that then, only strongly adsorbed proteins remain attached to the sensor. We found that the amount of strongly adsorbed proteins does not

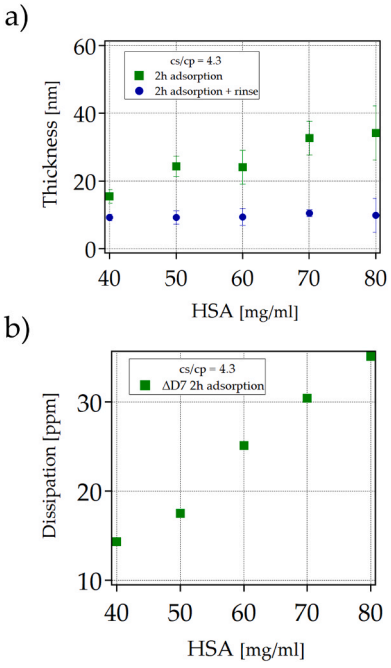

Fig. 2. Two hours of adsorption with constant c_s/c_p. a) Layer thickness of adsorbed and strongly adsorbed proteins and b) dissipation of multilayer before rinse.

change significantly with different protein concentration, and corresponds to one to two layers of strongly adhered proteins [31].

These properties, thick and less tightly (reversibly bound, since that they can be rinsed off), are characteristic for the enhanced adsorption found for HSA with $LaCl_3$, in contrast to a normal protein adsorption where usually the layer is stiffer and only one to two layers of proteins are adsorbed [31].

To investigate the correlation between protein adsorption and crystallization behavior, we measured the crystal nucleation density. We found that the number of crystals and their size increase with protein concentration (near c^*), see Tab. 1 (crystals counted after 9 days), additional data is given on Fig. S3. The increasing crystal nucleation density at higher protein concentrations correlates with enhanced adsorption and softer layers (Fig. 2), suggesting that such layer properties have a beneficial impact on the nucleation of protein crystals. Our data show that below a certain critical protein concentration c_p no HSA crystals are forming – despite the presence of irreversibly bound proteins on the substrate. This indicates that the crystals preferably start to grow within the layer of reversibly bound proteins.

2.3. Protein crystals at the interface

To further investigate whether crystallization occurs in the bulk solution or at the interface, optical microscopy, confocal microscopy and grazing-incidence small angle X-rays scattering (GISAXS) were performed. In order to investigate if the crystals are present at the solution or attached to the container wall, the protein-salt solution was extracted from the container after crystallization. Microscopy images were obtained from the container wall and the solution separately. We found that crystals are only present at the container vial walls (Fig. S4a)) and no crystal was visible at the solution. Additionally, a flow experiment showed that the crystals are strongly attached to the surface. During 30 min of solvent flux only partial dissolution of the crystal is visible, and no displacement or detachment took place (Fig. S4b)).

GISAXS confirmed the presence of crystalline material at the surface. In Fig. 3a), a GISAXS image exhibits distinct Bragg peaks from HSA crystals at the solid-liquid interface. The positions of the Bragg peaks, $|q| = (q_y^2 + q_z^2)^{1/2}$, are in good agreement with the crystal structure of HSA in the presence of another trivalent salt (YCl_3) [11]. Additionally, the widths of the Bragg peaks are related to the crystalline domain size. We found that in this system the domains are from 0.2 μm to 1 μm in size. Considering the crystal length (from 336 μm to 854 μm) measured from the confocal microscopy images (Tab. S1), we conclude that they are not single crystals, but oligocrystallites, consisting of several different crystalline domains. Moreover, by analyzing the accumulated scattering pattern from several GISAXS measurements (Fig. 3b)), an essentially random orientation of the crystalline domains with respect to the surface was found.

To eliminate any sedimentation influence, we also used the hanging drop method [38], where the glass surface is placed above the solution and not below it. We find that the crystals formed are attached to the surface (Fig. S5). This method showed that the observed crystals nucleate at the surface without sedimentation influence and that those

Table 1
Crystal density after 9 days, at a certain protein concentration (c_p) and salt concentration (c_s) normalized to maximum number of observed crystals, and the average size of the crystals.

protein concentration (mg/ml)	salt concentration (mM)	crystal density (a.u.)	average size (μm)
5	0.5	0	–
20	2	3	93
50	4.5	25	468
80	7	78	559
100	9	100	642

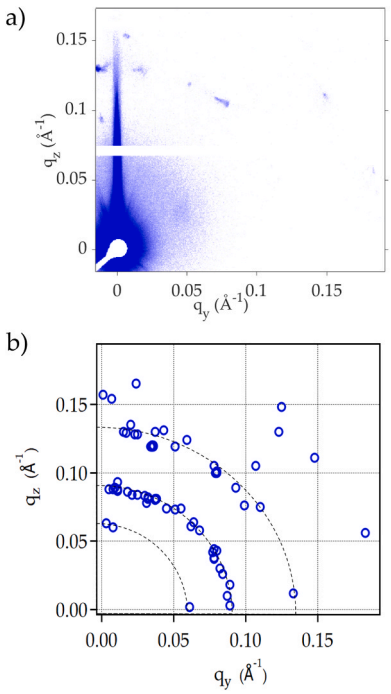

Fig. 3. a) a single GISAXS image showing distinct Bragg peaks originating from HSA crystals on the surface. Position of Bragg peaks confirm the presence of crystalline material at the surface. b) Bragg peaks from 27 GISAXS images. Dashed lines highlight the (002), (011) and (102) Debye-Scherrer rings of HSA-$LaCl_3$ crystals and correspond to the following lattice parameters: $a = 51.7$ Å, $b = 73.3$ Å, $c = 206.0$ Å, $\alpha = \beta = \gamma = 90°$ (space group $P2_12_12_1$).

crystals do not form in the bulk solution and then precipitate onto the surface, as this is not possible in this experimental setup. Thus, the sedimentation of material might influence the kinetics of the observed crystallization process, however it is not a necessary step for nucleation and crystal growth to occur.

To further test the hypothesis that crystals nucleate from the multilayer, confocal microscopy was performed. The intrinsic fluorescence of HSA [39] was used to image the three-dimensional shape of HSA crystals. Confocal microscopy images are shown in Fig. 4, revealing a macroscopic crystal shape that can be described as flat at the bottom with a oblate shape. The flat bottom was observed for all 20 crystals imaged, and indicates that the growth process starts from the adsorbed multilayer and continuous with supply from the adsorbed material and the solution. Additional images are given in Fig. S6.

3. Discussion

In this section, we discuss first protein adsorption and crystallization while highlighting the properties of the multilayer that may impact crystal nucleation. Then, we discuss a simplified mechanism of interface-assisted nucleation.

3.1. Enhanced adsorption, nucleation and crystal growth

The adsorption behavior of acidic globular proteins on a negatively charged surface (SiO_2) in the presence of trivalent salts was previously investigated by our group [17,18,31,40]. Specifically in Ref. [31], a model of ion-activated attractive patchy particles subjected to an effective external wall potential explains the protein adsorption at a charged surface in the presence of multivalent salts.

Here, we connected HSA crystallization with adsorption: the crystal nucleation density correlates to higher adsorption and softer layers. Additionally, an enhanced adsorption is present before crystals are

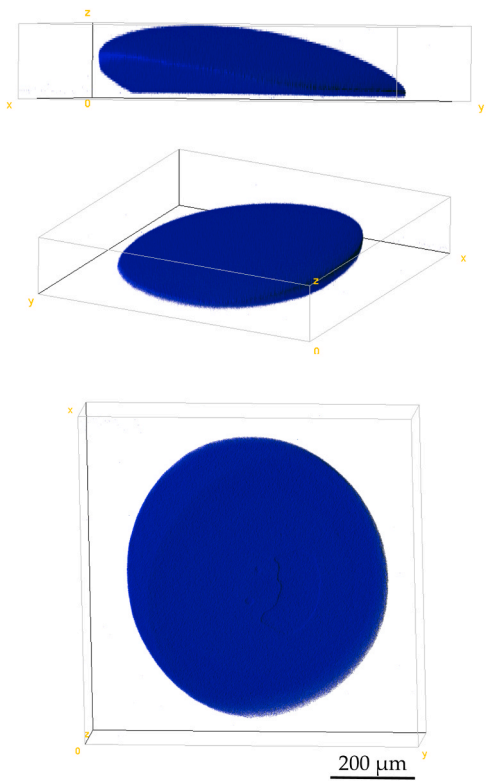

Fig. 4. Confocal *z*-stacks of an HSA crystal, three different views. The oblate crystal shape is flat at the bottom indicating a growth that starts at the interface and continuous with supply from the adsorbed material.

visible under the microscope, this behavior is consistent with wetting [31], and here it is shown to be preceding nucleation and crystal growth, for the conditions employed. This is consistent with Ref. [41], where the authors find a correlation between protein adsorption and crystallization density.

A thick and soft multilayer may have a role in triggering or serving as a precursor for crystal nucleation. The multilayer can act as a reservoir of molecules facilitating the nucleation of crystals [42–44], as the supersaturation is higher. Additionally, a soft and diffuse layer can allow protein rearrangements. Therefore, it may be favorable for proteins to assume orientations suitable for crystal nucleation [42,45,46].

After enhanced adsorption, two main features in the QCM-D response were detected before crystals are visible under the microscope: an anti-Sauerbrey behavior and an increase in dissipation. Both indicate a transformation within the multilayer. Additionally, we found that both features, frequency and dissipation changes, are characteristic to the crystallization behavior of two different proteins, suggesting that this response is rather universal to the crystallization behavior of proteins and not limited to HSA.

A transformation of the multilayer before crystals are visible suggests that the nucleation is happening within the adsorbed multilayer. To confirm this hypothesis, complementary techniques such as optical microscopy, GISAXS and confocal microscopy were employed. We find strong evidence of nucleation originating within the multilayer. This is in agreement with the theoretical background of nucleation. As heterogeneous nucleation, which occurs at foreign surfaces, has a lower energy barrier than homogeneous nucleation, making it more likely to occur [47].

3.2. Interface-assisted nucleation

We found that crystallization in this system is interface-assisted and that it takes place after enhanced adsorption. A schematic of this simplified mechanism is shown in Fig. 5. Here we discuss the involved steps.

In the first minutes adsorption of irreversibly bound proteins occurs, followed by enhanced adsorption of less tightly bound proteins. During the multilayer formation, changes in protein orientation may take place due to changes in the protein surroundings, such as continuous increase in protein density. In Ref. [48], the authors described a situation where proteins adsorb onto the surface assuming favorable surface-protein orientation and when adsorption continues, the protein density at the surface increases and protein-protein interactions become more relevant, triggering reorientation. This behavior is especially observed when the surface-protein interaction is of electrostatic nature [49].

In our system, the negatively charged surface can coordinate trivalent ions and a bridge forms between the surface and the protein through the trivalent ion [31]. This happens immediately after the salt addition and may favor a certain protein orientation to increase protein-surface interaction [49]. Afterwards, enhanced adsorption continues for many hours forming a multilayer of proteins due to the protein-protein interactions that are in the attractive regime, as described by the second virial coefficient. The increase in protein density at the surface might trigger rearrangements of the adsorbed proteins due to attraction or repulsion of the neighboring molecules. Additionally, this might be triggered only at a certain critical packing density at the surface [48,49], that is reached during the enhanced adsorption. This is consistent with the changes in dissipation observed during crystallization.

During enhanced adsorption the nucleation of crystals occurs. GISAXS measurements showed randomly oriented crystalline domains. We speculate that non-ideal growth conditions induce numerous crystal defects which result in randomly oriented crystalline domains.

In summary, rearrangements of proteins with a certain critical packing density might be necessary for the nucleation of crystals to occur. Specifically, within the multilayer, weakly bound proteins are adsorbed but can rearrange to assume different orientations, that are favorable for the nucleation of crystals [44,48]. This is in agreement with Ref. [44], where the authors state that the interaction of the protein with the surface has to be weak for rearrangements and then nucleation to occur. Additionally, a minimum critical packing density may also explain why at lower concentrations HSA does not crystallize. Since at low protein concentrations the thick and soft multilayer is not present, there are not enough weakly bound proteins to nucleate within the multilayer. Thus, enhanced adsorption followed by rearrangements of protein molecules within the multilayer due to protein-protein interactions, is a suitable explanation for the nucleation at the surface observed here.

4. Conclusion

We find that the nucleation of HSA crystals in the presence of a trivalent salt is interface-assisted. The mechanisms involved are a fast adsorption of irreversibly bound proteins followed by a longer time scale enhanced adsorption due to protein-protein interactions, of less tightly adsorbed proteins. These interactions become more relevant during time as adsorption continues, inducing protein rearrangements. The surface serves as a reservoir of protein molecules allowing optimal conditions for crystal nucleation and growth within the multilayer. Additionally, we find that the crystal density correlates with the layer thickness on the surface.

These findings highlight the importance of protein-surface interactions and possibly other interface-assisted phenomena for protein crystallization.

5. Materials and Methods

5.1. Materials and sample preparation

Albumin from human serum (HSA) with a purity ≥97 % (A9511) and

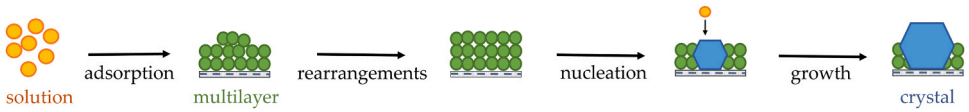

Fig. 5. Scheme depicting a simplified process from adsorption to crystallization. When the solution is in contact with the surface, a fast adsorption takes place and enhanced adsorption follows on a longer time scale. The data suggests a mechanism by which rearrangements take place within the multilayer. Then, protein crystals nucleate and grow. The multilayer can be considered as a dense phase at the surface.

$LaCl_3$ with a purity of 99.99 % (449830) were purchased from Merck. Stock solutions of salt and protein were prepared by dissolution in Milli-Q water. The concentration of the protein stock solution was determined by UV-Vis spectrophotometer measurements (Cary 50 UV-Vis spectrometer, Varian Technologies, USA) employing the Lambert-Beer law, the extinction coefficient for HSA is 0.531 ml/(mg · cm), at a wavelength of 278 nm where aromatic amino acids have an absorbance maximum. All samples were prepared by mixing Milli-Q water, protein stock solution and salt stock solution in glass vials at 21 ± 1 ˚C. No buffer was added as neutral trivalent salts (i.e. $LaCl_3$) do not induce significant pH variation [50,51].

5.2. Bulk phase behavior

The phase diagram of HSA with $LaCl_3$ was determined by visual inspection at protein concentrations c_p of 10, 30, 50 and 80 mg/ml varying the salt concentration c_s. Glass vials were used to mix the stock solution of protein with the stock solution of salt, achieving the final volume of 500 μm with the addition of water. At a fixed protein concentration $LaCl_3$ was added into the solution in a series of samples where the salt concentration was increased until the solution becomes visibly turbid. The first salt concentration where the solution is visibly turbid is indicated as the first pseudo phase boundary (c^*). After this turning point, the salt concentration was further increased until the second pseudo phase boundary (c^{**}) was reached, where the solution is visibly clear again. The second virial coefficient (B_2), was measured employing the method from Ref. [27].

5.3. Crystallization

Images of crystals were acquired using an optical microscope (Leica Microsystems, DM2700M, Germany), combined with the software ZEISS ZEN 3.2. The same software was used to process the images. Samples were prepared in glass vials and incubated for 4 days at RT. Images of HSA crystals attached to the walls of the glass vials were acquired. Afterwards, the total volume of the bulk liquid inside the vials was transferred onto microscope slides and images were acquired separately. Batch crystallization experiments for screening crystal density and crystal size were performed as follows: protein and salt were mixed at different concentrations on a eppendorf tube, water was added to achieve the desired volume. 25 μl of the freshly mixed solution was placed on a glass slide, the solution was covered with a glass cover slip, sealed with silicon. The hanging drop method was used to image protein crystals without sedimentation influence [38]. A hermetically closed petri dish was used to place the reservoir consisting of 400 μl of water with 5 mM of salt. One drop containing 85 mg/ml of protein with 5 mM of salt with a volume of 200 μl was placed in the uncoated glass surface at the top of the well. Crystals were imaged 24 h after sample preparation. 5 samples of the same protein and salt concentration were prepared.

A water flux measurement was performed inside the QCM-D chamber after protein crystallization. Water was pumped into the chamber for 30 min to test the crystal attachment to the solid-liquid interface. A peristaltic pump (Ismatec Reglo Digital Pump IPC ISM935C) was used with a flow rate of 1 ml/min and optical microscopy images were simultaneously acquired.

5.4. Confocal microscopy

Z-stacked images of HSA crystals on glass slides were acquired, employing a confocal fluorescence microcope (Leica TCS SP8 AOBS) with a 10x objective and an excitation laser wavelength of 488 nm and emission of 494–574 nm. With a detector HyD at 273 % gain. As tryptophan (Trp) 214 residue of HSA presents intrinsic fluorescence [39], no additional dye was used. The software ImageJ was employed to process the images.

5.5. X-ray scattering

Experiments to observe Bragg peaks at the interface were performed on a laboratory instrument (Xenocs, Xeuss 2.0, France) employing a GeniX 3D microfocus X-ray tube with a copper anode, producing X-rays with the wavelength of 1.54 Å. The GISAXS pattern were collected at the incident angle of 0.2˚ with a 2D detector (DECTRIS PILATUS 3R 300 K) placed at the distance 1644 mm from the sample. Samples were prepared as follows: the protein-salt mixture was added onto a cleaned flat SiO_2 substrate and hermetically closed in a well. The samples were kept at 21 ± 1 ˚C for 4 days. After the incubation time, the substrate without the bulk liquid was placed in the instrument chamber in an air environment. The acquired data was analyzed with the software GIXSGUI.

5.6. QCM-D

QCM-D is the main technique used in this study to analyze protein interface behavior under crystallization conditions. It is a real-time technique that utilizes acoustic waves generated by an oscillating piezoelectric single crystal quartz plate to analyze surface-interaction phenomena over solid interfaces. A quartz (ATcut) is placed between two gold electrodes and a mechanical oscillation of characteristic frequency is excited on the quartz by applying an alternated voltage [32]. When a change of mass occurs at the surface of the sensor (i.e. adsorption), a frequency shift (Δf) is recorded. In addition, QCM-D also measures changes in dissipation (ΔD), providing information about the viscoelastic properties of the adsorbed layer.

A QCM-D instrument (Biolin Scientific, Q-Sense Explorer, Sweden) was used to perform protein crystallization and adsorption experiments. A flow cell that provides optical access to the sensor surface through a sapphire window was used (Biolin Scientific, QWM401, Sweden). The setup was coupled with the optical microscope to follow the crystallization over the sensor in real-time. Images were acquired and analyzed with the software ZEISS ZEN 3.2. The QCM-D measurements were acquired and analyzed with the software QSoft and Dfind (Biolin Scientific, Sweden), respectively. SiO_2-coated flat sensors (5 MHz) (Quantum Design, QS-QSX303, Germany) were used as substrate. The viscoelastic Voigt model [52–54] was employed to extract the layer properties with the following parameters: protein layer density 1200 g/L, bulk density 1020 g/L and bulk viscosity 1.3 mPa · s.

The experiments were performed as follows: The chamber was filled with water for calibration and to define a baseline. After recording a stable baseline, the sample was freshly prepared and 400 μl was pumped into the cell containing 100 μl of solution above the sensor. The measurements were done at the controlled temperature of 20 ˚C. Simultaneously, microscopy images of the surface sensor were acquired during crystallization experiments. For crystallization experiments 6

repetitions were done for different protein and salt concentration. Adsorption experiments were carried out for the following protein concentrations: 40, 50, 60, 65, 70, 80, 85, 90, 100 mg/ml with several different salt concentrations.

CRediT authorship contribution statement

Alexander Gerlach: Writing – review & editing, Supervision, Methodology, Formal analysis, Data curation, Conceptualization. **Cara Buchholz:** Writing – review & editing, Investigation. **Ivan A. Zaluzhnyy:** Writing – review & editing, Data curation. **Furio Surfaro:** Writing – review & editing, Methodology, Formal analysis, Data curation, Conceptualization. **Kai-Florian Pastryk:** Writing – review & editing, Investigation. **Hadra Banks:** Writing – original draft, Supervision, Methodology, Formal analysis, Data curation, Conceptualization. **Frank Schreiber:** Writing – review & editing, Supervision, Resources, Project administration, Funding acquisition, Conceptualization.

Declaration of Competing Interest

The authors declare the following financial interests/personal relationships which may be considered as potential competing interests: Frank Schreiber reports financial support was provided by German Research Foundation. If there are other authors, they declare that they have no known competing financial interests or personal relationships that could have appeared to influence the work reported in this paper.

Data availability

Data will be made available on request.

Acknowledgement

The authors gratefully acknowledge funding by the DFG (Deutsche Forschungsgemeinschaft, SCHR 700/39-1). We acknowledge Ralf Zenke for the assistance in the confocal microscopy experiments.

Appendix A. Supporting information

Supplementary data associated with this article can be found in the online version at doi:10.1016/j.colsurfb.2024.114063.

References

[1] S. Assenza, R. Mezzenga, Soft condensed matter physics of foods and macronutrients, Nat. Rev. Phys. 1 (2019) 551.
[2] S. Hong, D.W. Choi, H.N. Kim, C.G. Park, W. Lee, H.H. Park, Protein-based nanoparticles as drug delivery systems, Pharmaceutics (2020) 12.
[3] F. Chiti, C.M. Dobson, Protein misfolding, amyloid formation, and human disease: a summary of progress over the last decade, Ann. Rev. Biochem. 86 (2017) 27.
[4] C. Sotomayor-Vivas, E. Hernández-Lemus, R. Dorantes-Gilardi, Linking protein structural and functional change to mutation using amino acid networks, PloS One 17 (2022) e0261829.
[5] Z. Dauter, A. Wlodawer, Progress in protein crystallography, Protein Pept. Lett. 23 (2016) 201.
[6] D. Fusco, P. Charbonneau, Soft matter perspective on protein crystal assembly, Colloids Surf. B: Biointerfaces 137 (2016) 22.
[7] F. Zhang, R. Roth, M. Wolf, F. Roosen-Runge, M.W.A. Skoda, R.M.J. Jacobs, M. Stzucki, F. Schreiber, Charge-controlled metastable liquid-liquid phase separation in protein solutions as a universal pathway towards crystallization, Soft Matter 8 (2012) 1313.
[8] A. Sauter, F. Roosen-Runge, F. Zhang, G. Lotze, R.M.J. Jacobs, F. Schreiber, Real-time observation of nonclassical protein crystallization kinetics, J. Am. Chem. Soc. 137 (2015) 1485.
[9] F. Zhang, Nonclassical nucleation pathways in protein crystallization, J. Phys. Condens. Matter 29 (2017) 443002.
[10] C.N. Nanev, Recent experimental and theoretical studies on protein crystallization, Cryst. Res. Technol. 52 (2017) 1600210.
[11] R. Maier, G. Zocher, A. Sauter, S. DaVela, O. Matsarskaia, R. Schweins, M. Sztucki, F. Zhang, T. Stehle, F. Schreiber, Protein Crystallization in the Presence of a Metastable Liquid-Liquid Phase Separation, Cryst. Growth Des. 20 (2020) 7951.
[12] C. Buchholz, L.F. Reichart, F. Surfaro, R. Maier, F. Zhang, A. Gerlach, F. Schreiber, Kinetics of HSA crystallization and its relationship with the phase diagram, J. Cryst. Growth 603 (2023) 126959.
[13] G. Falini, S. Fermani, G. Conforti, A. Ripamonti, Protein crystallisation on chemically modified mica surfaces, Acta Crystallogr. D. 58 (2002) 1649.
[14] F. Zhang, J.A. Gavira, G.W. Lee, D. Zahn, Nonclassical Nucleation–Role of Metastable Intermediate Phase in Crystal Nucleation: An Editorial Prefix, Crystals 11 (2021) 174.
[15] J.A. van Meel, A.J. Page, R.P. Sear, D. Frenkel, Two-step vapor-crystal nucleation close below triple point, J. Chem. Phys. 129 (2008) 204505.
[16] S. Curry, H. Mandelkow, P. Brick, N. Franks, Crystal structure of human serum albumin complexed with fatty acid reveals an asymmetric distribution of binding sites, Nat. Struct. Biol. 5 (1998) 827.
[17] R. Maier, M.R. Fries, C. Buchholz, F. Zhang, F. Schreiber, Human versus Bovine Serum Albumin: A Subtle Difference in Hydrophobicity Leads to Large Differences in Bulk and Interface Behavior, Cryst. Growth Des. 21 (2021) 5451.
[18] M.R. Fries, M.W.A. Skoda, N.F. Conzelmann, R.M.J. Jacobs, R. Maier, N. Scheffczyk, F. Zhang, F. Schreiber, Bulk phase behaviour vs interface adsorption: Effects of anions and isotopes on β -lactoglobulin (BLG) interactions, J. Colloid Interface Sci. 598 (2021) 430.
[19] G.J. Quinlan, G.S. Martin, T.W. Evans, Albumin: Biochemical properties and therapeutic potential, Hepatology 41 (2005) 1211.
[20] F. Fogolari, L. Ragona, S. Licciardi, S. Romagnoli, R. Michelutti, R. Ugolini, H. Molinari, Electrostatic properties of bovine β -lactoglobulin, Protein.: Struct., Funct., Bioinf 39 (2000) 317.
[21] F. Zhang, F. Roosen-Runge, A. Sauter, M. Wolf, R.M.J. Jacobs, F. Schreiber, Reentrant condensation, liquid-liquid phase separation and crystallization in protein solutions induced by multivalent metal ions, Pure Appl. Chem. 86 (2014) 191.
[22] F. Zhang, M.W.A. Skoda, R.M.J. Jacobs, S. Zorn, R.A. Martin, C.M. Martin, G. F. Clark, S. Weggler, A. Hildebrandt, O. Kohlbacher, F. Schreiber, Reentrant Condensation of Proteins in Solution Induced by Multivalent Counterions, Phys. Rev. Lett. 101 (2008) 148101.
[23] F. Roosen-Runge, F. Zhang, F. Schreiber, R. Roth, Ion-activated attractive patches as a mechanism for controlled protein interactions, Sci. Rep. 4 (2014) 7016.
[24] O. Matsarskaia, F. Roosen-Runge, F. Schreiber, Multivalent ions and biomolecules: Attempting a comprehensive perspective, ChemPhysChem 21 (2020) 1742.
[25] B.L. Neal, D. Asthagiri, O.D. Velev, A.M. Lenhoff, E.W. Kaler, Why is the osmotic second virial coefficient related to protein crystallization? J. Cryst. Growth 196 (1999) 377.
[26] A. George, Y. Chiang, B. Guo, A. Arabshahi, Z. Cai, W.W. Wilson, Meth. Enzymol, vol. 276, Academic Press, 1997, p. 100.
[27] F. Surfaro, R. Maier, K.-F. Pastryk, F. Zhang, F. Schreiber, R. Roth, An alternative approach to the osmotic second virial coefficient of protein solutions and its application to liquid-liquid phase separation, J. Chem. Phys. (2023) 158.
[28] C.J. Roberts, T.K. Das, E. Sahin, Predicting solution aggregation rates for therapeutic proteins: Approaches and challenges, Int. J. Pharm. 418 (2011) 318.
[29] A. George, W.W. Wilson, Predicting protein crystallization from a dilute solution property, Acta Crystallogr. D. 50 (1994) 361.
[30] G.A. Vliegenthart, H.N.W. Lekkerkerker, Predicting the gas-liquid critical point from the second virial coefficient, J. Chem. Phys. 112 (2000) 5364.
[31] M.R. Fries, D. Stopper, M.W.A. Skoda, M. Blum, C. Kertzscher, A. Hinderhofer, F. Zhang, R.M.J. Jacobs, R. Roth, F. Schreiber, Enhanced protein adsorption upon bulk phase separation, Sci. Rep. 10 (2020) 10349.
[32] C. Tonda-Turo, I. Carmagnola, G. Ciardelli, Quartz Crystal Microbalance With Dissipation Monitoring: A Powerful Method to Predict the in vivo Behavior of Bioengineered Surfaces, Front. Bioeng. Biotechnol. (2018) 6.
[33] M.B. Hovgaard, M. Dong, D.E. Otzen, F. Besenbacher, Quartz crystal microbalance studies of multilayer glucagon fibrillation at the solid-liquid interface, Biophys. J. 93 (2007) 2162.
[34] S. Kravchenko, B. Snopok, Vanishing mass" in the Sauerbrey world: quartz crystal microbalance study of self-assembled monolayers based on a tripod-branched structure with tuneable molecular flexibility, Analyst 145 (2020) 656.
[35] B.P. Regmi, J. Monk, B. El-Zahab, S. Das, F.R. Hung, D.J. Hayes, I.M. Warner, A novel composite film for detection and molecular weight determination of organic vapors, J. Mater. Chem. 22 (2012) 13732.
[36] U. Latif, S. Can, O. Hayden, P. Grillberger, F.L. Dickert, Sauerbrey and anti-Sauerbrey behavioral studies in QCM sensors—Detection of bioanalytes, Sens. Actuators B Chem. 176 (2013) 825.
[37] G. Dunér, E. Thormann, A. Dėdinaitė, Quartz Crystal Microbalance with Dissipation (QCM-D) studies of the viscoelastic response from a continuously growing grafted polyelectrolyte layer, J. Colloid Interface Sci. 408 (2013) 229.
[38] M.A. Dessau, Y. Modis, Protein crystallization for X-ray crystallography, J. Vis. Exp. (2011).
[39] M. Amiri, K. Jankeje, J.R. Albani, Origin of Fluorescence Lifetimes in Human Serum Albumin. Studies on Native and Denatured Protein, J. Fluoresc. 20 (2010) 651.
[40] M.R. Fries, D. Stopper, M.K. Braun, A. Hinderhofer, F. Zhang, R.M.J. Jacobs, M.W. A. Skoda, H. Hansen-Goos, R. Roth, F. Schreiber, Multivalent-Ion-Activated Protein Adsorption Reflecting Bulk Reentrant Behavior, Phys. Rev. Lett. 119 (2017) 228001.
[41] S. Glassford, K.L.A. Chan, B. Byrne, S.G. Kazarian, Chemical Imaging of Protein Adsorption and Crystallization on a Wettability Gradient Surface, Langmuir 28 (2012) 3174.
[42] A.K. Buell, in: M. Sandal (Ed.), International Review of Cell and Molecular Biology, Academic Press, 2017, p. 187. Vol. 329.

[43] Y.-Z. Guo, et al., Utilisation of adsorption and desorption for simultaneously improving protein crystallisation success rate and crystal quality, Sci. Rep. 4 (2014) 7308.
[44] G. Tosi, S. Fermani, G. Falini, J.A. Gavira Gallardo, J.M. Garcia Ruiz, Crystallization of proteins on functionalized surfaces, Acta Crystallogr. D. 64 (2008) 1054.
[45] A. Khaleghi, S.M. Sadrameli, M. Manteghian, Thermodynamic and kinetics investigation of homogeneous and heterogeneous nucleation, Rev. Inorg. Chem. 40 (2020) 167.
[46] G. Tosi, S. Fermani, G. Falini, J.A. Gavira, J.M. Garcia Ruiz, Hetero- vs Homogeneous Nucleation of Protein Crystals Discriminated by Supersaturation, Cryst. Growth Des. 11 (2011) 1542.
[47] X.Y. Liu, Heterogeneous nucleation or homogeneous nucleation? J. Chem. Phys. 112 (2000) 9949.
[48] M. Rabe, D. Verdes, S. Seeger, Understanding protein adsorption phenomena at solid surfaces, Adv. Colloid Interface Sci. 162 (2011) 87.
[49] Y.R. Dahal, M. Olvera de la Cruz, Controlling protein adsorption modes electrostatically, Soft Matter 16 (2020) 5224.
[50] M.R. Fries, N.F. Conzelmann, L. Günter, O. Matsarskaia, M.W.A. Skoda, R.M. J. Jacobs, F. Zhang, F. Schreiber, Bulk Phase Behavior vs Interface Adsorption: Specific Multivalent Cation and Anion Effects on BSA Interactions, Langmuir 37 (2021) 139.
[51] F. Roosen-Runge, B.S. Heck, F. Zhang, O. Kohlbacher, F. Schreiber, Interplay of pH and Binding of Multivalent Metal Ions: Charge Inversion and Reentrant Condensation in Protein Solutions, J. Phys. Chem. B 117 (2013) 5777.
[52] A.D. Easley, T. Ma, C.I. Eneh, J. Yun, R.M. Thakur, J.L. Lutkenhaus, A practical guide to quartz crystal microbalance with dissipation monitoring of thin polymer films, J. Polym. Sci. 60 (2022) 1090.
[53] R. van der Westen, P.K. Sharma, H. De Raedt, I. Vermue, H.C. van der Mei, H. J. Busscher, Elastic and viscous bond components in the adhesion of colloidal particles and fibrillated streptococci to QCM-D crystal surfaces with different hydrophobicities using Kelvin-Voigt and Maxwell models, Phys. Chem. Chem. Phys. 19 (2017) 25391.
[54] S.X. Liu, J.-T. Kim, Application of Kelvin–Voigt Model in Quantifying Whey Protein Adsorption on Polyethersulfone Using QCM-D, J. Assoc. Lab. Autom. 14 (2009) 213.